

# Original research article

## Physico-chemical characterization and estimation of antimicrobial activity of modified aspirin in the form of nano-organometallic compounds

### Abstract:

Aspirin is one of the most commonly used drugs. It is necessary to find and develop analgesic anti-inflammatory drugs that are safe against their adverse effects. From this standpoint, new nano-organometallic Cu(II), Mn(II), Ni(II), Cd(II) and Zn(II) compounds of modified aspirin were prepared and characterized using elemental and spectroscopic techniques such as infrared and ultraviolet, proton nuclear magnetic resonance, mass spectroscopy, electron spin resonance and electron microscope, as well as magnetism, conductivity and thermal analysis. Thermal and spectral results showed the octahedral geometry and stability of these compounds up to 45°C. The data indicated that, using low concentration against microbes, aspirin and ligand no effect was observed, however, the complexes showed moderate to high effect, The order for Gram positive is Cd(II) complex (10) > Cd(II) complex (11) > ampicillin > Zn(II) complex (8) > Cu(II) complex (4) > Cu(II) complex (6) = Ni(II) complex (12) > Cu(II) complex (2) = Cu(II) complex (3) > ligand (1) > aspirin > Mn(II) complex (14) and for Gram negative is ampicillin > Cd(II) complex (10) > Cd(II) complex (11) > Cu(II) complex (2) > Cu(II) complex (6) > Cu(II) complex (3) > Cu(II) complex (4) > Zn(II) complex (8) > aspirin > Ni(II) complex (12) > ligand (1) > Mn(II) complex (14) and for *Aspergillus flavus* is Cd(II) complex (10) > amphotericin B > Cd(II) complex (11) > ligand (1) = aspirin = Cu(II) complex (2) = Cu(II) complex (3) = Cu(II) complex (4) = Cu(II) complex (6) = Zn(II) complex (8) = Ni(II) complex (12) = Mn(II) complex (14) and for *Candida albicans* is Cd(II) complex (10) > Cd(II) complex (11) > amphotericin B > Ni(II) complex (12) > Cu(II) complex (3) = Cu(II) complex (6) > Cu(II) complex (2) = Cu(II) complex (4) > ligand (1) = aspirin = Zn(II) complex (8) = Mn(II) complex (14). The order of the catalytic effect of the tested complexes on decomposition of H<sub>2</sub>O<sub>2</sub> was Mn(II) complex (14) > Ni(II) complex (12) > Cu(II) complex (4) > Cu(II) complex (6) > Cu(II) complex (2) respectively.

### Keywords:-

Nano-organometallic compounds, elemental analysis, spectra, magnetism, antimicrobial activity, catalytic activity.

### Introduction:-

In recent decades, the chemistry of metal(II) carboxylate complexes, especially N donor ligands [1, 2]. Some transition metal complexes have broad biological activities, such as analgesic, anti-inflammatory, antibacterial, and antiviral properties, and can act as anticancer agents, enzyme inhibitors, and chemical

nucleases [3, 4]. The introduction of metal ions or components that bind metal ions to biological systems for the treatment of diseases is one of the major branches of bioinorganic chemistry [5]. The intentional introduction of metal ions into human biological systems is useful for diagnostic and therapeutic purposes. The role of antibiotic metal complexes (AMCs) in modern pharmacy continues to expand. New, more effective and broad-acting drugs must be found [6]. Complexes of metal ions with antibiotics offer great opportunities in this regard. The main reason is that many drugs change their pharmacological and toxicological properties when they appear in the form of metal complexes [7-11]. Aspirin is a commonly used antipyretic, analgesic and anti-inflammatory agent [12]. Due to their reactivity as precursors for further modifications via their corresponding carboxyl groups, there is an increasing demand for aspirin and its derivatives for various biological properties [13]. Aspirin derivatives have shown antibacterial activity against *Bacillus subtilis*, *Escherichia coli*, *Staphylococcus aureus* and *Pseudomonas aeruginosa* [14, 15]. Other important biological properties of aspirin derivatives have been reported for anticancer, antitumor, antifungal and antibacterial properties [16, 17]. Urea (chemical formula:  $\text{CH}_4\text{N}_2\text{O}$ ), also known as carbamide, is a hygroscopic polar molecule [18]. The importance of urea in dermatology is twofold: it mainly has a key physiological role in maintaining skin hydration and secondarily it has been used for more than a century in various topical preparations and concentrations in various skin conditions. One of the first uses of urea was in the topical treatment of wounds due to its antibacterial and proteolytic properties [19]. The importance of urea in the treatment of wound healing has diminished as it has been overtaken by the development of more specific and effective drugs, while its use as a moisturizer and keratolytic agent became more popular. Several studies of the use of urea in the treatment of xerosis, atopic dermatitis, ichthyosis, psoriasis and other conditions generally use low concentrations as a general emollient on the face and body and higher concentrations on thickened areas of skin. Where rapid and keratolytic action is required [20]. Another field of growing interest has been the association of urea with other active ingredients, such as topical corticosteroids [21] and antifungals [22] in order to improve its penetration into the skin. This article presents the current topic for the preparation and characterization of new nanoorganometallic compounds from modified aspirin hopping for new antimicrobial drug discovery.

## **EXPERIMENTAL:**

### **• Materials**

The starting chemicals were of analytical grade and used without further purification.

### **• Physical and spectroscopic techniques**

The characterization of the ligand and its metal complexes was carried out using various elemental and spectroscopic techniques such as:- Elemental analyses (C, H, N and Cl) were performed by the analytical laboratory of the University of Cairo, in Egypt.

### **Molar conductivity:**

The molar conductivity of  $10^{-3}$  M of compounds in dimethyl-sulfoxide (DMSO) was determined using a Bibby conductometer MCI at room temperature. Molar conductivities were calculated using the following equation:

$$\Lambda_M = V * K * g / M_w * \Omega$$

Where:  $\Lambda_M$  = molar conductivity ( $\text{ohm}^{-1}\text{cm}^2\text{mol}^{-1}$ ) V = volume of the solution ( $100\text{ cm}^3$ )

K = cell constant:  $0.92\text{ cm}^{-1}$

$M_w$  = molecular weight of the complex

g = grams of complex dissolved in  $100\text{ cm}^3$  solution

$\Omega$  = resistance measured in ohms

### **• Mass spectra:**

The mass spectra of the compounds were recorded on JEOL JMS-XA- 500 mass spectrometer.

### **• Thermal analyses:**

DTA and TGA were performed on a Shimadzu DT-30 thermal analyzer in nitrogen atmosphere, from room temperature to  $600\text{ }^\circ\text{C}$  at a heating rate of  $10\text{ }^\circ\text{C}$  per minute.

### **• $^1\text{H-NMR}$ spectra:**

The  $^1\text{H}$ -NMR spectra were recorded on a JEOL EX-270 MHz FT-NMR spectrometer in deuterated dimethylsulfoxide (DMSO - $d^6$ ) as a solvent. The chemical shifts were measured with respect to the solvent peaks.

- **IR spectra:**

The infrared spectra of the ligand and its complexes were recorded on Perkin Elmer's infrared spectrometer 681 using KBr or CsBr discs.

- **Electronic absorption spectra:**

The electronic absorption spectra of the compounds were recorded on UNICO SQ-4802 UV/Vis. Double beam spectrophotometer (190- 1100 nm) using a 1 cm quartz cell with DMSO as a solvent.

- **Magnetic susceptibility**

The magnetic susceptibilities of the solid compounds at room temperature were measured in a borosilicate tube with a Johnson Matthey at room temperature using the following equations:

$$X_a = [2.086 L (R - R^0) / (10^9 W)]$$

$$X_m = X_a * M_w$$

$$X_n = X_m - D$$

$$\mu_{\text{eff}} = 2.828 (X_n \times T)^{1/2} \text{ Where:-}$$

$X_a$  = mass susceptibility  $L$  = sample length in cm

$R$  = tube + sample reading  $R^0$  = empty the reading

$W$  = mass of the sample  $X_m$  = molar susceptibility  $M_w$  = molecular weight

$X_n$  = corrected molar susceptibility  $D$  = diamagnetic corrections

$\mu_{\text{eff}}$  = effective magnetic moment  $T$  = room temperature in Kelvin.

- **Characterization of transmission electron microscopy (TEM)**

TEM samples for colloidal suspension of Cd(II) complex(**10**) in distilled water were prepared by dropping the colloids onto carbon-coated TEM grids and allowing the liquid carrier to evaporate in air then assayed by a JEOL JEM-1230 Electron Microscope.

- **Determination of the metal content**

The metal content was determined using the colorimetric method on the HACH DR 5000 spectrophotometer [23-25].

- **ESR spectra**

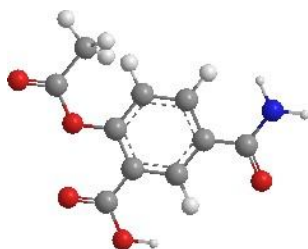
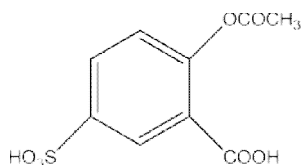
The solid ESR spectra of some complexes were recorded at room temperature using ELEXSYS E500 Bruker spectrometer in 3 nm Pyrex Tubes at 25°C. Diphenylpicryl-hydrazide (DPPH) free radical was used as a g- maker for the calibration of the spectra. The equation used to determine g- values was

$$g = (g_{\text{DPPH}} (H_{\text{DPPH}}) / H \text{ Where: } g_{\text{DPPH}} = 2.0036$$

$H_{\text{DPPH}}$  = magnetic field of DPPH in gauss  $H$  = magnetic field of the sample in gauss.

- **Preparation of the ligand (1) :**

It was prepared by reflux with stirring for 2 hours, (2-acetoxy-5-sulfobenzoic acid) (30.00 g, 3.597 mol) dissolved in 30 cm<sup>3</sup> ethanol with (urea) (6.08 ml, 3.374 mol). The formed product was allowed to cool to room temperature to give the final ligand (2-acetoxy-5-carbamoylbenzoic acid). The preparation of the ligand (**1**) is shown in **Scheme 1**.



### Scheme (1): Preparation of the ligand (1)

Ligand (1): Yield 97%; m.p. 150 ; color is pink ; Anal. Calcd. for  $C_9H_{10}O_8S$  (FW=223): C, 53.50; H, 4.00; N, 6.20. Found (%) C, 53.81; H, 4.04; N, 6.28, IR (KBr,  $cm^{-1}$ ), 3413  $\nu(OH)$ , 1616  $\nu(CONH_2)$ , 1660  $\nu(C=O)$  acetyl, 1704  $\nu(C=O)$  carboxylic; The mass spectrum of the ligand (1) revealed molecular ion peak at  $m/z$  223. The analytical data for ligand (1) and its complexes are shown in Table (1):-

#### • Preparation of metal complexes (2)-(15) :

The metal complexes (2-15) were prepared by refluxing with stirring an appropriate quantity of a hot ethanolic solution of the following metal salts:  $Cu(OAc)_2 \cdot 3H_2O$  (1.60 g, 0.108 mol) complex (2),  $Cu(OAc)_2 \cdot H_2O$  (0.80 g, 0.039 mol) complex (3),  $CuSO_4 \cdot 5H_2O$  (1.12 g, 0.076 mol) complex (4),  $CuSO_4 \cdot 5H_2O$  (0.56 g, 0.028 mol) complex (5),  $CuCl_2 \cdot 2H_2O$  (1.20 g, 0.089 mol) complex (6),  $CuCl_2 \cdot 2H_2O$  (0.60 g, 0.003 mol) complex (7),  $Zn(OAc)_2 \cdot 3H_2O$  (1.97 g, 0.132 mol) complex (8),  $Zn(OAc)_2 \cdot 3H_2O$  (0.98 g, 0.048 mol) complex(9),  $Cd(OAc)_2 \cdot 3H_2O$  (2.39 g, 0.147 mol) complex(10),  $Cd(OAc)_2 \cdot 3H_2O$  (1.20 g, 0.055 mol) complex(11),  $Ni(OAc)_2 \cdot 4H_2O$  (2.23 g, 0.152 mol) complex(12),  $Ni(OAc)_2 \cdot 4H_2O$  (1.12 g, 0.055 mol) complex(13),  $Mn(OAc)_2 \cdot 4H_2O$  (2.20 g, 0.151 mol) complex(14),  $Mn(OAc)_2 \cdot 4H_2O$  (1.10g, 0.055 mol) complex(15) with a hot ethanolic solution of the ligand (1) (1.50 ml, 0.2242 mol). The ligand and metal ions used were used at molar ratios of 1L: 1M and 2L: 1M in  $30\text{ cm}^3$  of ethanol for periods of 1-3 hours. The precipitates which formed were filtered off, washed with ethanol then with diethyl ether and dried over  $P_4O_{10}$  in a desiccator under vacuum.

- **Biological activity**
- **Antimicrobial activity (invitro study):**

The antimicrobial activity of the tested compounds was evaluated against Gram positive bacteria (*Staphylococcus aureus*), Gram negative bacteria (*Escherichia coli*) and Fungi (*Aspergillus flavus*) and (*Candida albicans*) using the disc diffusion method [26]. Ampicillin was used as a positive control for bacteria and amphotericin B for fungi and solvent control (DMSO) was also used to learn about solvent activity. Test compounds were dissolved in DMSO to give concentrations of 250, 200, 175, 150 and 125 ppm and a DMSO poured disc was used as negative control. The bacteria were subcultured into agar nutrient medium prepared with peptone, beef extract, NaCl, agar and distilled water. The Petri dishes were incubated for 48 hours at 37 °C. Standard antimicrobial drugs have also been screening in similar conditions for comparison. The inhibition zone has been measured carefully in millimeters. All determination was made in duplication for each of the compounds. An average of the two independent readings for each compound was registered.

- **Invivo studies (Toxicity study):**

Toxicity study of cadmium(II) complex (**10**) with molecular weight equal to 543 and chemical formula  $C_{14}H_{25}O_{14}CdN$  was done. The complex was dissolved in DMSO diluted with sterile saline 0.9% NaCl to a maximum concentration of 0.2% by volume for intraperitoneal injection.

#### **Animals:**

Twenty healthy male albino rats, 8 weeks old (180-200 g) were purchased from the National Cancer Institute, Cairo, Egypt. The rats were housed in temperature-controlled cages (22- 25°C). They were kept with good ventilation under a 12hour light/12hour dark photoperiod with the lights on from 06:00 to 18:00. They were all fed standard laboratory food (60% ground cornmeal, 10% bran, 15% ground beans, 10% corn oil, 3% casein, 1% mixed minerals and 1% vitamin mix), purchased from Meladco Feed Company (Obour City, Cairo, Egypt) and watered ad libitum throughout the experiment.

#### **Experimental design:**

Twenty animals were given 10 days for to adapt. They were then randomly divided into 2 equal groups, 10 rats each. The groups of animals were recognized as follows:

**Group 1 (control):** normal healthy control animals.

**Group 2:** Each animal was injected intraperitoneally with  $1 \times 10^{-5}$  mmole/L Cd(II) complex (**10**) for 6 weeks.

#### **Blood collection**

At the end of the experimental period (6 weeks), blood samples were collected from overnight rats, centrifuged at 3000 rpm for 10 minutes and the separated sera were frozen at -20 °C for future biochemical analysis.

#### **Biochemical analyses**

The activities of liver enzymes, aspartate aminotransferase (AST) and alanine aminotransferase (ALT) were estimated using kinetic kits purchased from Human Diagnostic Kits, Germany [27]. Liver function, albumin concentration and kidney functions, blood urea and serum creatinine were measured with the Diamond Diagnostic kits, Egypt. All biochemical analyzes were determined using a Biosystems BTS-310 spectrophotometer [28].

#### **Hematological analyses**

An automated hemogram was done in all cases. This included hemoglobin estimation, red cell count, white blood cells, and platelet count.

These parameters were obtained electronically by colter counter model Beckman 750 Int, U.S.A.

#### **Statistical analysis**

Data were tested for statistical significance using one-way analysis of variance (ANOVA), followed by Duncan's multiple range test. Statistical analysis was performed using SPSS 16.00 software. The results were expressed as mean  $\pm$  SE and the differences were considered significant at  $P \leq 0.05$  [29].

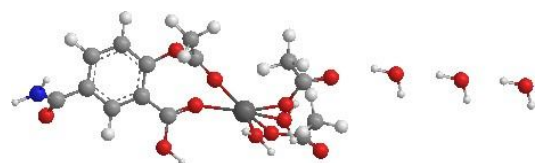
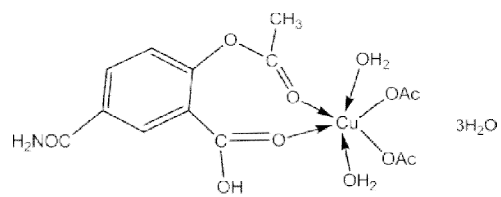
## Results and discussion:

Ligand (1) and its metal complexes (2)-(15) are stable at room temperature, non-hydroscopic and are insoluble in common solvents such as ethanol, acetone, water, and chloroform, but soluble in DMF and DMSO. Elemental analysis confirmed that all complexes are composed of the ligand and metal ions with molar ratios of 1L:1M, and 2L:1M. Many attempts have been made to grow a single crystal, but unfortunately they have failed so far. Some of the metal complexes are found in nano form with a size range of (5.65 to 11.50 nm) and explain different properties of these complexes. Analytical, physical and spectral data are presented in the experimental part and Tables (1) to (6) which consistent with the proposed structures as shown in Fig (1).

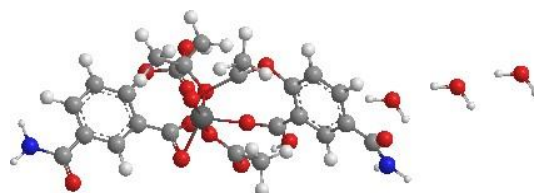
**Table 1:- Analytical and physical data of the ligand (1) and its metal complexes.**

No.	Ligand/Complexes	Color	FW	M.P ( <sup>o</sup> C)	Yield (%)	Anal. /Found (Calc.) (%)				Conductivity Λ
						C	H	N	M	
(1)	[HL] C <sub>10</sub> H <sub>9</sub> O <sub>5</sub> N	Off white	223	150	97	53.50 (53.81)	4.00 (4.04)	6.20 (6.28)	-	-
(2)	[(HL)Cu(OAc) <sub>2</sub> (H <sub>2</sub> O) <sub>2</sub> ].3H <sub>2</sub> O C <sub>14</sub> H <sub>25</sub> O <sub>14</sub> Cu N	Olive green	494	310	95	33.80 (33.97)	5.20 (5.06)	2.75 (2.83)	12.75 (12.84)	11.50
(3)	[(HL) <sub>2</sub> Cu(OAc) <sub>2</sub> ].3H <sub>2</sub> O C <sub>24</sub> H <sub>30</sub> O <sub>17</sub> Cu N <sub>2</sub>	Olive green	681	312	93	33.30 (33.46)	4.45 (4.40)	4.00 (4.11)	9.20 (9.32)	11.00
(4)	[(HL)Cu(H <sub>2</sub> O) <sub>4</sub> ].SO <sub>4</sub> .2H <sub>2</sub> O C <sub>10</sub> H <sub>21</sub> O <sub>15</sub> Cu S N	Blue	490	315	90	24.40 (24.46)	4.65 (4.28)	2.70 (2.85)	12.60 (12.95)	103
(5)	[(HL) <sub>2</sub> Cu(SO <sub>4</sub> )(H <sub>2</sub> O)].3H <sub>2</sub> O C <sub>20</sub> H <sub>26</sub> O <sub>18</sub> Cu S N <sub>2</sub>	Sky blue	677	320	92	35.30 (35.42)	3.70 (3.84)	4.05 (4.13)	9.35 (9.37)	13.2
(6)	[(HL)Cu(Cl) <sub>2</sub> (H <sub>2</sub> O) <sub>2</sub> ].3H <sub>2</sub> O C <sub>10</sub> H <sub>19</sub> O <sub>10</sub> Cu Cl <sub>2</sub> N	Dark green	447	322	85	26.20 (26.82)	4.70 (4.25)	3.23 (3.13)	15.50 (15.87)	12.60
(7)	[(HL) <sub>2</sub> Cu(Cl) <sub>2</sub> ].3H <sub>2</sub> O C <sub>20</sub> H <sub>24</sub> O <sub>13</sub> Cu Cl <sub>2</sub> N <sub>2</sub>	Light green	634	325	87	37.35 (37.83)	3.50 (3.78)	4.30 (4.41)	10.15 (10.01)	13.00
(8)	[(HL)Zn(OAc) <sub>2</sub> (H <sub>2</sub> O) <sub>2</sub> ].3H <sub>2</sub> O C <sub>14</sub> H <sub>25</sub> O <sub>14</sub> Zn N	Simon	496	333	90	33.45 (33.85)	5.35 (5.04)	2.70 (2.82)	13.40 (13.16)	13.50
(9)	[(HL) <sub>2</sub> Zn(OAc) <sub>2</sub> ].3H <sub>2</sub> O C <sub>24</sub> H <sub>30</sub> O <sub>17</sub> Zn N <sub>2</sub>	Pink	683	335	86	42.77 (42.15)	4.57 (4.39)	4.25 (4.10)	9.50 (9.56)	13.80
(10)	[(HL)Cd(OAc) <sub>2</sub> (H <sub>2</sub> O) <sub>2</sub> ].3H <sub>2</sub> O C <sub>14</sub> H <sub>25</sub> O <sub>14</sub> Cd N	Simon	543	314	84	30.99 (30.94)	4.69 (4.60)	2.40 (2.58)	20.45 (20.70)	13.00
(11)	[(HL) <sub>2</sub> Cd(OAc) <sub>2</sub> ].3H <sub>2</sub> O C <sub>24</sub> H <sub>30</sub> O <sub>17</sub> Cd N <sub>2</sub>	Pink	730	313	80	39.28 (39.43)	4.61 (4.11)	3.66 (3.83)	15.51 (15.39)	13.20
(12)	[(HL)Ni(OAc) <sub>2</sub> (H <sub>2</sub> O) <sub>2</sub> ].3H <sub>2</sub> O C <sub>14</sub> H <sub>25</sub> O <sub>14</sub> Ni N	Olive green	489	338	81	34.35 (34.31)	5.71 (5.11)	2.65 (2.86)	11.56 (11.97)	14.00
(13)	[(HL) <sub>2</sub> Ni(OAc) <sub>2</sub> ].3H <sub>2</sub> O C <sub>24</sub> H <sub>30</sub> O <sub>17</sub> Ni N <sub>2</sub>	Grey	676	340	83	33.98 (33.70)	4.52 (4.43)	4.00 (4.14)	8.45 (8.66)	14.60
(14)	[(HL)Mn(OAc) <sub>2</sub> (H <sub>2</sub> O) <sub>2</sub> ].3H <sub>2</sub> O C <sub>14</sub> H <sub>25</sub> O <sub>14</sub> Mn N	Off white	485	328	94	34.86 (34.58)	5.68 (5.15)	2.54 (2.88)	11.43 (11.30)	14.50
(15)	[(HL) <sub>2</sub> Mn(OAc) <sub>2</sub> ].3H <sub>2</sub> O C <sub>24</sub> H <sub>30</sub> O <sub>17</sub> Mn N <sub>2</sub>	Beige	673	330	95	42.55 (42.80)	4.60 (4.46)	4.32 (4.16)	8.20 (8.16)	15.00

\* m<sup>-1</sup> cm<sup>2</sup> mol<sup>-1</sup>



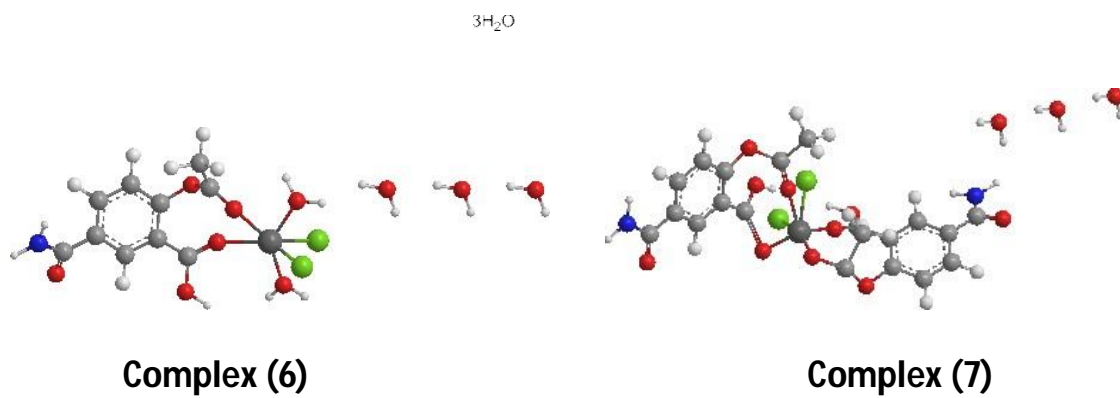
**Complex (2)**



**Complex (3)**

**Complex (4)**

**Complex (5)**

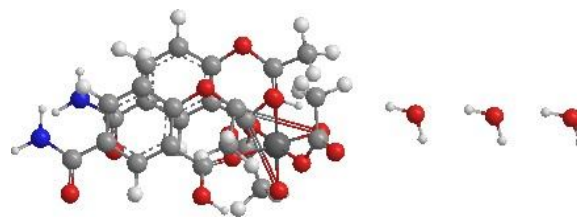
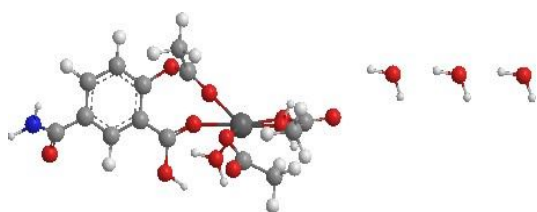


**Complex (8)**

**Complex (9)**

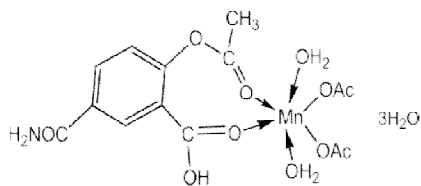
**Complex (10)**

**Complex (11)**



**Complex (12)**

**Complex (13)**



**Complex (14)**

**Complex (15)**

**Figure (1): proposed structures of the ligand (1) and its metal complexes**

### **Characterization of transmission electron microscopy (TEM)**

TEM images were obtained for the colloidal suspensions of Cd(II) complex (10). The average diameter of this spherical Cd(II) complex (10) was proved to be (5.65 –11.50) nm as shown in the figure (2).

**Figure (2): Electromicroscopic diagram of complex (10)**

- **Molar Conductivity**

The molar conductivities of the  $1 \times 10^{-3}$  M solutions of the complexes in DMSO at room temperature are in the range (11.00-15.00)  $\text{ohm}^{-1} \text{cm}^2 \text{mol}^{-1}$  indicating the non-electrolytic in nature of all the complexes with the exception of the complex complex (4) indicates the value is  $103 \text{ Ohm}^{-1} \text{cm}^2 \text{mol}^{-1}$ ,confirming the electrolytic nature. These low values correspond to the coordination of anions to metal ions [30].

### Mass Spectra of Ligand [HL] and some of its metal complexes:

The mass spectrum of ligand (1) [HL], (Table (2, a)) showed the molecular ion peak at  $m/z$  223 amu, confirming its formula weight (F.W. 223). The patterns of mass fragmentation observed at  $m/z = 53, 79, 119, 149, 183$  and 223 amu correspond to  $C_3HO, C_5H_3O, C_8H_7O, C_8H_7O_2N, C_8H_9O_4N$  and  $C_{10}H_9O_5N$  moieties, respectively, supporting the proposed structure of the ligand.

**Table (2, a): Mass spectrum of the ligand (1):**

Ligand (1)	$m/z$	Rel. Int.	Fragment
	53	27	$C_3HO$
	79	32	$C_5H_3O$
	119	23	$C_8H_7O$
	149	22	$C_8H_7O_2N$
	183	21	$C_8H_9O_4N$
	223	15	$C_{10}H_9O_5N$

The mass spectrum of complex (2) (Table (2, b)) showed the molecular ion peak at  $m/z$  494 amu, confirming its formula weight (F.W. 494). The patterns of mass fragmentation observed at  $m/z = 55, 57, 71, 85, 149, 197, 249, 318, 398, 414, 465$  and 494 amu correspond to  $C_3H_3O, C_5H_5O, C_4H_7O, C_5H_9O, C_5H_{10}OCu, C_5H_{10}O_4Cu, C_8H_{10}O_5Cu, C_8H_{15}O_9Cu, C_8H_{15}O_{14}Cu, C_8H_{17}O_{14}NCu, C_{12}H_{20}O_{14}NCu$  and  $C_{14}H_{25}O_{14}NCu$  moieties, respectively, supporting the proposed structure of the complex.

**Table (2, b): Mass spectrum of the Cu(II) complex (2):**

Complex	$m/z$	Rel. Int.	Fragment
(2)	55	83	$C_3H_3O$
	57	100	$C_5H_5O$
	71	55	$C_4H_7O$
	85	34	$C_5H_9O$
	149	35	$C_5H_{10}OCu$
	197	41	$C_5H_{10}O_4Cu$
	249	51	$C_8H_{10}O_5Cu$
	318	23	$C_8H_{15}O_9Cu$
	398	24	$C_8H_{15}O_{14}Cu$
	414	21	$C_8H_{17}O_{14}NCu$
	465	31	$C_{12}H_{20}O_{14}NCu$
	494	17	$C_{14}H_{25}O_{14}NCu$

The mass spectrum of **complex (3)** (Table (2, c)) showed the molecular ion peak at  $m/z$  681 amu, confirming its formula weight (F.W. 681). The patterns of mass fragmentation observed at  $m/z$  = 55, 71, 97, 149, 199, 293, 387, 465, 544, 625 and 681 amu correspond to  $C_3H_3O$ ,  $C_3H_3O_2$ ,  $C_5H_5O_2$ ,  $C_8H_7O_2N$ ,  $C_{11}H_7O_2N_2$ ,  $C_{12}H_9O_7N_2$ ,  $C_{14}H_{16}O_7N_2Cu$ ,  $C_{15}H_{18}O_{11}N_2Cu$ ,  $C_{16}H_{21}O_{15}N_2Cu$ ,  $C_{20}H_{22}O_{17}N_2Cu$  and  $C_{24}H_{30}O_{17}N_2Cu$  moieties, respectively, supporting the proposed structure of the complex.

**Table (2, c): Mass spectrum of the Cu(II) complex (3):**

Complex	$m/z$	Rel. Int.	Fragment
(3)	55	44	$C_3H_3O$
	71	22	$C_3H_3O_2$
	97	22	$C_5H_5O_2$
	149	28	$C_8H_7O_2N$
	199	21	$C_{11}H_7O_2N_2$
	293	100	$C_{12}H_9O_7N_2$
	387	21	$C_{14}H_{16}O_7N_2Cu$
	465	41	$C_{15}H_{18}O_{11}N_2Cu$
	544	51	$C_{16}H_{21}O_{15}N_2Cu$
	625	19	$C_{20}H_{22}O_{17}N_2Cu$
	681	15	$C_{24}H_{30}O_{17}N_2Cu$

The mass spectrum of **complex (8)** (Table (2, d)) showed the molecular ion peak at  $m/z$  496 amu, confirming its formula weight (F.W. 496). The patterns of mass fragmentation observed at  $m/z$  = 55, 71, 85, 98, 129, 149, 205, 295, 356, 412, 467 and 496 amu correspond to  $C_3H_3O$ ,  $C_3H_3O_2$ ,  $C_4H_5O_2$ ,  $C_5H_6O_2$ ,  $C_5H_7O_3N$ ,  $C_5H_{11}O_4N$ ,  $C_7H_{11}O_6N$ ,  $C_9H_{12}O_6NZn$ ,  $C_{10}H_{13}O_9NZn$ ,  $C_{12}H_{13}O_{11}NZn$ ,  $C_{12}H_{20}O_{14}NZn$  and  $C_{14}H_{25}O_{14}NZn$  moieties, respectively, supporting the proposed structure of the complex.

**Table (2, d): Mass spectrum of the Zn(II) complex (8):**

Complex	m/z	Rel. Int.	Fragment
(8)	55	33	C <sub>3</sub> H <sub>3</sub> O
	71	29	C <sub>5</sub> H <sub>3</sub> O <sub>2</sub>
	85	20	C <sub>4</sub> H <sub>5</sub> O <sub>2</sub>
	98	51	C <sub>5</sub> H <sub>6</sub> O <sub>2</sub>
	129	100	C <sub>5</sub> H <sub>7</sub> O <sub>3</sub> N
	149	61	C <sub>5</sub> H <sub>11</sub> O <sub>4</sub> N
	205	41	C <sub>7</sub> H <sub>11</sub> O <sub>6</sub> N
	295	45	C <sub>9</sub> H <sub>12</sub> O <sub>6</sub> NZn
	356	31	C <sub>10</sub> H <sub>13</sub> O <sub>9</sub> NZn
	412	22	C <sub>12</sub> H <sub>13</sub> O <sub>11</sub> NZn
	467	21	C <sub>12</sub> H <sub>20</sub> O <sub>14</sub> NZn
	496	17	C <sub>14</sub> H <sub>25</sub> O <sub>14</sub> NZn

The mass spectrum of **complex (11)** (Table (2, e)) showed the molecular ion peak at  $m/z$  730 amu, confirming its formula weight (F.W. 730). The patterns of mass fragmentation observed at  $m/z$  = 55, 70, 86, 98, 129, 143, 200, 316, 401, 505, 609, 674 and 730 amu correspond to C<sub>3</sub>H<sub>3</sub>O, C<sub>3</sub>H<sub>4</sub>ON, C<sub>3</sub>H<sub>4</sub>O<sub>2</sub>N, C<sub>4</sub>H<sub>4</sub>O<sub>2</sub>N, C<sub>4</sub>H<sub>5</sub>O<sub>3</sub>N<sub>2</sub>, C<sub>5</sub>H<sub>7</sub>O<sub>3</sub>N<sub>2</sub>, C<sub>7</sub>H<sub>8</sub>O<sub>5</sub>N<sub>2</sub>, C<sub>7</sub>H<sub>12</sub>O<sub>5</sub>N<sub>2</sub>Cd, C<sub>7</sub>H<sub>17</sub>O<sub>10</sub>N<sub>2</sub>Cd, C<sub>14</sub>H<sub>21</sub>O<sub>11</sub>N<sub>2</sub>Cd, C<sub>21</sub>H<sub>25</sub>O<sub>12</sub>N<sub>2</sub>Cd, C<sub>21</sub>H<sub>26</sub>O<sub>16</sub>N<sub>2</sub>Cd and C<sub>24</sub>H<sub>30</sub>O<sub>17</sub>N<sub>2</sub>Cd moieties, respectively, supporting the proposed structure of the complex.

**Table (2, e): Mass spectrum of the Cd(II) complex (11):**

Complex	m/z	Rel. Int.	Fragment
(11)	55	77	C <sub>3</sub> H <sub>3</sub> O
	70	49	C <sub>3</sub> H <sub>4</sub> ON
	86	31	C <sub>3</sub> H <sub>4</sub> O <sub>2</sub> N
	98	26	C <sub>4</sub> H <sub>4</sub> O <sub>2</sub> N
	129	100	C <sub>4</sub> H <sub>5</sub> O <sub>3</sub> N <sub>2</sub>
	143	19	C <sub>5</sub> H <sub>7</sub> O <sub>3</sub> N <sub>2</sub>
	200	16	C <sub>7</sub> H <sub>8</sub> O <sub>5</sub> N <sub>2</sub>
	316	51	C <sub>7</sub> H <sub>12</sub> O <sub>5</sub> N <sub>2</sub> Cd
	401	25	C <sub>7</sub> H <sub>17</sub> O <sub>10</sub> N <sub>2</sub> Cd
	505	41	C <sub>14</sub> H <sub>21</sub> O <sub>11</sub> N <sub>2</sub> Cd
	609	23	C <sub>21</sub> H <sub>25</sub> O <sub>12</sub> N <sub>2</sub> Cd
	674	22	C <sub>21</sub> H <sub>26</sub> O <sub>16</sub> N <sub>2</sub> Cd
730	21	C <sub>24</sub> H <sub>30</sub> O <sub>17</sub> N <sub>2</sub> Cd	

The mass spectrum of **complex (13)** (**Table (2, f)**) showed the molecular ion peak at  $m/z$  676 amu, confirming its formula weight (F.W. 676). The patterns of mass fragmentation observed at  $m/z = 55, 71, 85, 98, 129, 149, 199, 293, 391, 454, 529, 613$  and 676 amu correspond to C<sub>3</sub>H<sub>3</sub>O, C<sub>3</sub>H<sub>3</sub>O<sub>2</sub>, C<sub>3</sub>H<sub>3</sub>O<sub>2</sub>N, C<sub>4</sub>H<sub>4</sub>O<sub>2</sub>N, C<sub>4</sub>H<sub>5</sub>O<sub>3</sub>N<sub>2</sub>, C<sub>4</sub>H<sub>9</sub>O<sub>4</sub>N<sub>2</sub>, C<sub>8</sub>H<sub>11</sub>O<sub>4</sub>N<sub>2</sub>, C<sub>9</sub>H<sub>13</sub>O<sub>9</sub>N<sub>2</sub>, C<sub>11</sub>H<sub>13</sub>O<sub>10</sub>N<sub>2</sub>Ni, C<sub>12</sub>H<sub>16</sub>O<sub>13</sub>N<sub>2</sub>Ni, C<sub>18</sub>H<sub>19</sub>O<sub>13</sub>N<sub>2</sub>Ni, C<sub>21</sub>H<sub>19</sub>O<sub>16</sub>N<sub>2</sub>Ni and C<sub>24</sub>H<sub>30</sub>O<sub>17</sub>N<sub>2</sub>Ni moieties, respectively, supporting the proposed structure of the complex.

**Table (2, f): Mass spectrum of the Ni(II) complex (13):**

Complex	m/z	Rel. Int.	Fragment
(13)	55	53	C <sub>3</sub> H <sub>3</sub> O
	71	28	C <sub>3</sub> H <sub>3</sub> O <sub>2</sub>
	85	28	C <sub>3</sub> H <sub>3</sub> O <sub>2</sub> N
	98	91	C <sub>4</sub> H <sub>4</sub> O <sub>2</sub> N
	129	25	C <sub>4</sub> H <sub>5</sub> O <sub>3</sub> N <sub>2</sub>
	149	21	C <sub>4</sub> H <sub>9</sub> O <sub>4</sub> N <sub>2</sub>
	199	100	C <sub>8</sub> H <sub>11</sub> O <sub>4</sub> N <sub>2</sub>
	293	81	C <sub>9</sub> H <sub>13</sub> O <sub>9</sub> N <sub>2</sub>
	391	29	C <sub>11</sub> H <sub>13</sub> O <sub>10</sub> N <sub>2</sub> Ni
	454	27	C <sub>12</sub> H <sub>16</sub> O <sub>13</sub> N <sub>2</sub> Ni
	529	51	C <sub>18</sub> H <sub>19</sub> O <sub>13</sub> N <sub>2</sub> Ni
	613	24	C <sub>21</sub> H <sub>19</sub> O <sub>16</sub> N <sub>2</sub> Ni
	676	17	C <sub>24</sub> H <sub>30</sub> O <sub>17</sub> N <sub>2</sub> Ni

The mass spectrum of **complex (15)** (Table (2, g)) showed the molecular ion peak at  $m/z$  673 amu, confirming its formula weight (F.W. 673). The patterns of mass fragmentation observed at  $m/z = 55, 80, 98, 129, 149, 167, 200, 232, 293, 375, 480, 584$  and 673 amu correspond to C<sub>3</sub>H<sub>3</sub>O, C<sub>5</sub>H<sub>4</sub>O, C<sub>5</sub>H<sub>6</sub>O<sub>2</sub>, C<sub>5</sub>H<sub>7</sub>O<sub>3</sub>N, C<sub>5</sub>H<sub>11</sub>O<sub>4</sub>N, C<sub>5</sub>H<sub>13</sub>O<sub>5</sub>N, C<sub>5</sub>H<sub>14</sub>O<sub>7</sub>N, C<sub>5</sub>H<sub>14</sub>O<sub>9</sub>N, C<sub>10</sub>H<sub>15</sub>O<sub>9</sub>N, C<sub>10</sub>H<sub>19</sub>O<sub>13</sub>N<sub>2</sub>, C<sub>14</sub>H<sub>21</sub>O<sub>13</sub>N<sub>2</sub>Mn, C<sub>17</sub>H<sub>25</sub>O<sub>17</sub>N<sub>2</sub>Mn and C<sub>24</sub>H<sub>30</sub>O<sub>17</sub>N<sub>2</sub>Mn moieties, respectively, supporting the proposed structure of the complex.

**Table (2, g): Mass spectrum of the Mn(II) complex (15):**

Complex	m/z	Rel. Int.	Fragment
(15)	55	100	C <sub>3</sub> H <sub>3</sub> O
	80	90	C <sub>5</sub> H <sub>4</sub> O
	98	25	C <sub>5</sub> H <sub>6</sub> O <sub>2</sub>
	129	27	C <sub>5</sub> H <sub>7</sub> O <sub>3</sub> N
	149	32	C <sub>5</sub> H <sub>11</sub> O <sub>4</sub> N
	167	51	C <sub>5</sub> H <sub>13</sub> O <sub>5</sub> N
	200	31	C <sub>5</sub> H <sub>14</sub> O <sub>7</sub> N
	232	29	C <sub>5</sub> H <sub>14</sub> O <sub>9</sub> N
	293	31	C <sub>10</sub> H <sub>15</sub> O <sub>9</sub> N
	375	21	C <sub>10</sub> H <sub>19</sub> O <sub>13</sub> N <sub>2</sub>
	480	23	C <sub>14</sub> H <sub>21</sub> O <sub>13</sub> N <sub>2</sub> Mn
	584	22	C <sub>17</sub> H <sub>25</sub> O <sub>17</sub> N <sub>2</sub> Mn
673	23	C <sub>24</sub> H <sub>30</sub> O <sub>17</sub> N <sub>2</sub> Mn	

- **IR Spectra**

The IR data of the ligand and its metal complexes are shown in Table (3). “The IR spectra of the ligand (1) showed a strong vibrational band at 1680 cm<sup>-1</sup> which was assigned to the carbonyl  $\nu$ (C=O) of the acetyl group, while the broad band which observed at 3413 cm<sup>-1</sup> was assigned to the stretching vibration of the aromatic hydroxyl group and the other band at 1616 cm<sup>-1</sup> was assigned to the stretching vibration of the  $\nu$ (CONH<sub>2</sub>) group. The broad bands appearing at 3560-3230 and 3220-2460 cm<sup>-1</sup> ranges were assigned to inter- and intramolecular hydrogen bondings” [31]. “These observations confirmed the presence of the ligand in in solid state ketone form” [32]. “The spectrum of the ligand also showed band at 1740 which can be assigned to  $\nu$ (C=O) of carboxyl group” [33]. “The bands appeared at 1421 and 772 cm<sup>-1</sup>, they were assigned to  $\nu$ (Ar) vibration. Comparing the IR spectral data of the complexes with those of the free ligand. Note that, in all complexes the appearance of a new band in the range of 1710-1669 cm<sup>-1</sup> which can be assigned to the C=O of carboxyl group and this band has shifted to a lower value, compromising the coordination of this group with the metal ion” [34]. “In the spectra of all complexes, the absorption frequency of  $\nu$ (C=O) of the acetyl group was shifted to the lower frequency side and appeared in the region of 1684-1623 cm<sup>-1</sup> with a decrease in its intensity, confirming the coordination

of the oxygen atom  $\nu(\text{C}=\text{O})$  of the acetyl group with the metal ions without undergoing enolization. It was also observed that, the presence of an absorption band due to a hydroxyl group appearing in the spectra of complexes in the range of  $(3460\text{-}3412)\text{ cm}^{-1}$  indicated that this group is not coordinated with the metal ion Table(3) [35]. “The appearance of new bands appeared in the  $623\text{-}588$ , and  $590\text{-}541\text{ cm}^{-1}$  ranges for different complexes can be assigned to the  $\nu(\text{M}-\text{O})$ ” [36]. “The results confirmed that, the bonding of the ligand with the metal ions tookplace via carbonyl oxygen of acetyl and carboxylic groups” [37]. “Strong bands appeared at  $3370$  and  $3210\text{ cm}^{-1}$  related to  $\nu(\text{NH}_2)$  respectively. The bands appeared at  $1578$  and  $1565\text{ cm}^{-1}$ , were assigned to  $\nu(\text{NH})$  vibration. The aromatic ring vibrations appeared in the  $(1482\text{-}1434)$  and  $(786\text{-}770)\text{ cm}^{-1}$  ranges. In the case of acetate complexes (**2,3**), (**8-15**) there are two new bands appeared in the  $1473\text{-}1380$  and  $1348\text{-}1333\text{ cm}^{-1}$  ranges which are attributed to the symmetric and asymmetric stretching vibration of the acetate group. The separation values ( $\Delta$ ) between  $\nu_{\text{asym}}(\text{COO}^-)$  and  $\nu_{\text{sym}}(\text{COO}^-)$  in these complexes suggest the coordination of the acetate group in as a monodentate fashion” [38]. “In the case of the sulfate complexes, new bands appeared at  $1216$ ,  $1175$ ,  $1031$ ,  $664$  for the complex (**4**) and  $1218$ ,  $1158$ ,  $1083$ ,  $664$  for the complex (**5**). These bands indicated that the sulfate ion is coordinated with the metal ion. In the case of the chloride complexes (**6**) and (**7**), new bands appeared respectively at  $445$  and  $442\text{ cm}^{-1}$ , suggesting the coordination of the chloride group with the metal ion. The appearance of broad bands in the range  $(1640\text{-}1610)\text{ cm}^{-1}$  is assigned to the stretching vibrations of the  $\nu(\text{CONH}_2)$  group. The appearance of broad bands in the ranges  $(3580\text{-}3210)$  and  $(3320\text{-}3080)\text{ cm}^{-1}$  are due to hydrated or coordinated water molecules” [39]. However, the hydrogen bondings appeared at  $(3650\text{-}3220)$  and  $(3330\text{-}2445)\text{ cm}^{-1}$  ranges. The above results together with elemental analyses indicated that, the ligand behaved as neutral bidentate fashion bonded to the metal ions through the carbonyl oxygen atoms of the acetyl and carboxylic groups.

**Table (3):- IR frequencies of the bands (cm<sup>-1</sup>) of the ligand (1) and its metal complexes:**

No.	$\nu(\text{H}_2\text{O})$	$\nu(\text{OH})$	$\nu(\text{H-bonding})$	$\nu(\text{C=O})$ Acetyl	$\nu(\text{C=O})$ carb	$\nu(\text{CONH}_2)$	$\nu(\text{NH}_2)$	$\nu(\text{C-O})$	$\nu(\text{C-N})$	$\nu(\text{NH})$	$\nu(\text{ON})$	$\nu(\text{Ar})$	$\nu(\text{OAc}/\text{SO}_4)$	$\nu(\text{M-O})$	$\nu(\text{M-Cl})$
(1)	-	3413	(3560-3230) , (3220-2460)	1660	1704	1616	3250, 3217	1128, 1080	1480	1570	-	(1421, 772)	-	-	-
(2)	(3550-3310) , (3300-3150)	3434	(3550-3260) , (3250-2720)	1635	1675	1615	3255, 3225	1123, 1032	1477	1571	1512	(1440, 770)	1380, 1335	610, 590	-
(3)	(3520-3310), (3300-3150)	3460	(3560-3250), (3240-2870)	1630, 1625	1670, 1655	1613	3300, 3265	1129, 1031	1473	1569	1509	(1445, 773)	1473,1341	604, 541	-
(4)	(3530-3220) , (3210-3135)	3412	(3600-3220), (3210-2560)	1682	1710	1616	3350, 3235	1144, 1089	1585	1572	1530	(1478, 773)	1216, 1175, 1031, 664	623, 589	-
(5)	(3530-3210) , (3200-3125)	3415	(3620-3220) , (3210-2465)	1650	1700, 1684	1618	3370, 3235	1129, 1031	1581	1568	1511	(1480, 773)	1218, 1158, 1083, 664	590, 575	-
(6)	(3530-3330) , (3320-3140)	3424	(3650-3310) , (3300-2485)	1684	1690	1640	3351, 3220	1128, 1031	1579	1565	1508	(1481, 773)	-	588, 575	445
(7)	(3520-3220) , (3210-3140)	3423	(3570-3280) , (3270-2445)	1644, 1635	1700, 1685	1620	3370, 3220	1129, 1031	1573	1572	1513	(1481, 773)	-	589, 570	442
(8)	(3520-3310) , (3300-3150)	3456	(3600-3320) , (3310-2780)	1632	1670	1615	3360, 3230	1128, 1033	1580	1569	1507	(1480, 772)	1444, 1335	595, 580	-
(9)	(3530-3310) , (3300-3135)	3457	(3570-3310) , (3300-2650)	1640	1675	1616	3361, 3210	1127, 1036	1582	1567	1508	(1482, 774)	1448, 1348	597, 530	-
(10)	(3530-3330) , (3320-3140)	3446	(3650-3310) , (3330-2750)	1623	1670	1610	3370, 3280	1126, 1034	1517	1568	1514	(1434, 774)	1438, 1335	598	-
(11)	(3530-3330) , (3320-3150)	3455	(3650-3310) , (3300-2750)	1623	1670	1613	3369, 3275	1126, 1036	1520	1578	1515	(1477, 775)	1451,1345	597	-
(12)	(3510-3310) , (3300-3100)	3457	(3620-3290) , (3280-2470)	1644	1671	1611	3365, 3235	1129, 1032	1587	1577	1510	(1479,774)	1441, 1333	601, 580	-
(13)	(3580-3350) , (3320-3090)	3449	(3615-3300) , (350-2450)	1648	1670	1617	3361, 3231	1129, 1035	1585	1572	1512	(1481, 777)	1442, 1347	595, 575	-
(14)	(3540-3320) , (3310-3100)	3438	(3610-3290) , (3210-2560)	1647	1673	1618	3362, 3236	1128, 1035	1586	1570	1513	(1482, 782)	1443, 1346	595, 571	-
(15)	(3530-3300) , (3290-3080)	3444	(3605-3270) , (3190-2580)	1643	1669	1611	3368, 3233	1127, 1034	1580	1571	1510	(1480, 786)	1440, 1348	595, 581	-

- **Magnetic Moments:**

“The magnetic moments of the metal complexes (2)-(15) at room temperature are shown in Table 4. The Cu(II) complexes (2), (3), (4), (5), (6) and (7) showed values between 1.68 and 1.70 B.M, corresponding to an unpaired electron in the a  $d_{(x^2-y^2)}$  ground state in an octahedral structure. The low values as low as 1.73 B.M are due to spin – spin interactions that have taken place between Cu(II) ions” [40]. The Mn(II) complexes (14) and (15) showed magnetic moments of 6.18 and 6.31 B.M. These values are lower than those of high spin manganese (II), ( $d^5$ ). This phenomenon may be due to antiferromagnetic spin-spin interactions between Mn(II) ions through by molecular association or hydrogen bonding [41]. Ni(II) complexes (12) and (13) showed values equal to 3.05 and 2.98 B.M. The lowering in these values may be assigned to the interaction between the two nickel atoms via hydrogen bondings or molecular association [42]. Zn(II) complexes (8) and (9), Cd(II) complexes (10) and (11) showed diamagnetic property [43].

- **Electronic spectra:**

“The electronic spectral data for the ligand (1) and its metal complexes in DMSO are summarized in Table 4. The electronic absorption spectra of the ligand showed three bands located at 295, 315 and 335 nm, respectively. The first one was assigned to the intraligand  $\pi \rightarrow \pi^*$  transition in the hydroxyl moiety, which remains almost unchanged upon complexation. The second and third bands may be assigned to  $n \rightarrow \pi^*$  and charge- transfer transitions of the carboxyl and carbonyl groups. It was found that the location of these bands is shifted to higher energy upon complexation. This finding gave the participation of these groups to binding and coordination with metal ions” [44]. “Copper(II) complexes (2), (3), (4), (5), (6) and (7) showed bands in the 296-265, 361-310, 463-435, 565-531 and 647-620 nm ranges, were assigned to intraligand transition  $O \rightarrow Cu$ , charge transfer,  ${}^2B_1 \rightarrow {}^2E$  and  ${}^2B_1 \rightarrow {}^2B_2$  transitions, indicating distorted octahedral structure” [45]. Manganese(II) complexes (14) and (15) showed bands at 282, 291, 314, 321, 337, 416, 528 and 621 and 285, 290, 312, 323, 335, 415, 55 and 623 nm, the first three bands are within the ligand and the other bands are corresponding to  ${}^6A_{g1} \rightarrow {}^4E_g$ ,  ${}^6A_{1g} \rightarrow {}^4T_{2g}$  and  ${}^6A_{1g} \rightarrow {}^4T_{1g}$  transitions which were compatible to an octahedral geometry around the Mn(II) ions [46]. However, the electronic spectra of nickel(II) complexes (12) and (13) showed bands at 282, 295, 325, 345, 405, 460, 548, 580 and 745 nm and 283, 298, 329, 347, 410, 461, 545, 582 and 747 nm, which were assignable to intraligand transitions and  ${}^3A_{2g}(F) \rightarrow {}^3T_{1g}(P)$  (3),  ${}^3A_{2g}(F) \rightarrow {}^3T_{1g}(F)$  (2) and  ${}^3A_{2g}(F) \rightarrow {}^3T_{1g}(F)$  (1) transitions respectively, assuming the octahedral Ni(II) complexes [47]. The  $(\nu_2/\nu_1)$  ratio for the complexes are less than the usual value 1.7 indicating distorted octahedral Ni(II) complexes, the  $(\nu_2/\nu_1)$  value equal to 1.58 and 1.53, which indicates a distorted octahedral structure. Zn(II) complexes (8) and (9) and Cd(II) complexes (10) and (11) showed bands were due to intraligand transitions.

**Table (4):- The electronic absorption spectral bands (nm) and magnetic moments (B.M.) for the ligand (1) and its metal complexes:**

No.	$\lambda_{\text{max}}$ (nm)	eff in B.M.	$\nu_2/\nu_1$
(1)	295nm (log $\epsilon$ =3.98), 315 nm ( log $\epsilon$ =4.25) 335(log $\epsilon$ = 4.59)	-	-
(2)	640, 556, 438, 361, 343, 324, 295, 266	1.70	-
(3)	642, 554, 435, 360, 341, 322, 292, 265	1.69	-
(4)	647, 531, 438, 349, 336, 326, 310, 293, 279	1.70	-
(5)	640, 559, 456, 347, 329, 295, 287	1.70	-
(6)	620, 560, 461, 355, 335, 316, 296, 290	1.68	-
(7)	625, 565, 463, 360, 340, 315, 291, 285	1.69	-
(8)	321, 307, 291	Diamagnetic	-
(9)	324, 305, 290	Diamagnetic	-
(10)	326, 303, 294	Diamagnetic	-
(11)	322, 306, 292	Diamagnetic	-
(12)	745, 580, 548, 460, 405, 345, 325, 295, 282	3.05	1.58
(13)	747, 582, 545, 461, 410, 347, 329, 298, 283	2.98	1.53
(14)	621, 528, 416, 337, 321, 314, 291, 282	6.18	-
(15)	623, 525, 415, 335, 323, 312, 290, 285	6.31	-

• **Electron Spin Resonance (ESR)**

“The ESR spectral data for copper (II) complexes (3), (5) and (6) are presented in Table 5. The spectra of copper (II) complexes are characteristic of species  $d^9$ , configuration with axial type at a  $d_{(x^2-y^2)}$  most common ground state for copper (II) complexes. The complexes showed  $g_{\parallel} > g_{\perp} > 2.0023$ , indicating octahedral geometry around the copper (II) ion. The g-values are related to the expression  $G = (g_{\parallel} - 2) / (g_{\perp} - 2)$ , where (G) exchange coupling interaction parameter (G). If  $G < 4.0$ , a significant exchange coupling is present, whereas if G value  $> 4.0$ , local tetragonal axes are aligned parallel or only slightly misaligned. The copper (II) Complexes showed values of 2.00, 2.61, and 2.7, indicating that spin-exchange interactions took place between the copper (II) ions. This phenomenon is further confirmed by the values of the magnetic moments (Table (4)). The  $g_{\parallel}/A_{\parallel}$  value is also used as a diagnostic term for stereochemistry, the  $g_{\parallel}/A_{\parallel}$  values are 155.7, 147.3 and 182.5 which are expected for distorted octahedral complexes” [48]. The g-values of copper(II) complexes with a  $^2B_{1g}$  ground state ( $g_{\parallel} > g_{\perp}$ ) can be expressed by.

$$g_{\parallel} = 2.002 - (8K^2 / \Delta E_{xy}) \quad (1)$$

$$g_{\perp} = 2.002 - (2K^2 / \Delta E_{xz}) \quad (2)$$



### Thermal Analyses (DTA and TGA):

Thermal data of complexes (2), (4), (5), (6), (7), (8), (9), (10), (12), (13) and (15) are listed in Table 6. These complexes are shown as representative examples. The thermogram of complex (2) showed a six-step decomposition six steps, the first involving H-bond breaking accompanied by an endothermic peak at 46 °C. In the second step, three molecules of hydrated water molecules were endothermically lost with a peak at 70°C accompanied by 10.90% (Calc. 10.93%) weight loss. Loss of two coordinated water molecule was recorded in the third step as an endothermic peak at 155 °C with 8.10% (Calc. 8.18%) weight loss. The 29.25% weight loss (Calc. 29.21%) accompanied by an endothermic peak at 270-285 °C range was assigned to loss of coordinated 2(OAc) group, whereas the endothermic peak observed at 310 °C referred to the melting point of the complex. The final step observed as exothermic peaks at 442,495,575 and 615°C with 27.70% weight loss (Calc. 27.80%), refers to complete decomposition of the exposed complex to form CuO. The first step observed in the thermogram of complex (4) involves the breaking of the H bond accompanied by an endothermic peak at 48°C. In the second step, two molecules of hydrated water were lost endothermically with a peak at 75°C accompanied by a weight loss of 7.30% (calculated 7.35%). In the third step, three molecules of coordinated water molecules were endothermically lost with a peak at 145 °C accompanied by 12.00% (calc. 11.89%) weight loss. The fourth step involved the loss of the coordinate group (SO<sub>4</sub>) accompanied by an endothermic peak in the region of 265°C with 24.10% (calculated 24.00%). while the endothermic peak appeared at 315 °C related to the melting point of the complex. The last step was observed at 475, 515, 590 and 605°C with a weight loss of 26.30% (calc. 26.15%) as exothermic peaks, referring to the complete oxidative decomposition of the complex which ends with the formation of CuO. The first step observed in the thermogram of the complex (5) involves breaking of H-bondings accompanied with endothermic peak at 50°C. In the second step, three molecules of hydrated water were lost endothermically with peak at 60 accompanied by 7.90% (Calc. 7.98%) weight loss. In the third step, one molecule of coordinated water molecules was lost endothermically with a peak at 150 °C accompanied by 2.80% (Calc. 2.89%) weight loss. The fourth step involved loss of coordinated (SO<sub>4</sub>) group accompanied with an endothermic peaks at 260, 290 °C ranges with 15.80% (Calc. 15.89%). while the endothermic peak appeared at 320 °C referred to the melting point of the complex. The final step observed at 430,465, 515 and 600°C with 15.60% weight loss (Calc. 15.62%) as exothermic peaks, referring to the complete oxidative decomposition of the complex which ends with the formation of CuO. Thermogram of complex (6) showed a six-step decomposition, the first step involving breaking of H-bondings accompanied with endothermic peak at 45 °C. In the second step, three molecules of hydrated water molecules were lost endothermically with peak at 80 °C accompanied by 12.00% (Calc. 12.08%) weight loss. Loss of one coordinated water molecule was recorded in the third step as an endothermic peak at 160 °C with 9.10% (Calc. 9.16%) weight loss. The 19.80% weight loss (Calc. 19.89%) accompanied by an endothermic peak at 270-285 °C range was assigned to loss of coordinated 2(Cl) group, whereas the endothermic peak observed at 322 °C referred to the melting point of the complex. The final step observed as exothermic peaks at 435,480,510 and 595°C with 27.75% weight loss (Calc. 27.80%), referred to complete decomposition of the complex which exposed up with the formation of CuO. The first step observed in the thermogram of complex (7) involving breaking of H-bondings accompanied with endothermic peak at 47 °C. In the second step, three molecules of hydrated water were lost endothermically with peak at 72 °C accompanied by 8.60% (Calc. 8.52%) weight loss. The 12.20% weight loss (Calc. 12.24%) accompanied by an endothermic peaks appear at 273-282°C was assigned to loss of coordinated 2(Cl) groups whereas the endothermic peak observed at 325 °C referred to the melting point of the complex. The final step observed at 470,535,600 and 610 °C with 15.50% weight loss (Calc. 15.62%), refers to complete oxidative decomposition of the complex which exposed up with the formation of CuO. The thermogram of complex (8) showed a six-step decomposition, the first involving H-bond breaking accompanied by an endothermic peak at 46 °C. In the second step, three molecules of hydrated water molecules were endothermically lost with a peak at 73°C accompanied by a weight loss of 10.80% (calculated 10.89%). The loss of two coordinated water molecules was recorded in the third step as an endothermic peak at 155°C with a weight loss of 8.10%

(calculated 8.14%). Weight loss of 29.10% (calculated 29.06%) accompanied by an endothermic peak in a range of 260-275 °C was attributed to the loss of coordinated group 2 (OAc), while the endothermic peak observed at 333 °C is related to the melting point of the complex. The last passage observed as exothermic peaks at 420, 480, 530 and 615 °C with a weight loss of 28.20% (calc. 28.13%), related to the complete decomposition of the exposed complex with the formation of ZnO. The thermogram of complex (9) showed a five-step decomposition, with the first step involving the breaking of the H bonds accompanied by an endothermic peak at 49 °C. In the second step, three molecules of hydrated water molecules were endothermically lost, with a peak at 80°C, accompanied by a weight loss of 7.90% (calculated 7.91%). The weight loss of 18.70% (calculated 18.76%) accompanied by an endothermic peak in the range of 275-280 °C was attributed to loss of coordinated group 2(OAc), while the observed endothermic peak at 335 °C indicated the melting point of the complex. The final step, observed as exothermic peaks at 445, 490, 545 and 600 °C with a weight loss of 15.80% (calculated 15.85%), was related to complete decomposition of the complex, which exposed to the formation of ZnO. The thermogram of complex (10) showed a six-step decomposition, the first involving the breaking of the H bonds accompanied by an endothermic peak at 45 °C. In the second phase, three molecules of hydrated water were lost endothermally with a peak at 60 °C accompanied by a weight loss of 9.90% (Calc. 9.94%). The loss of two coordinated water molecules was recorded in the third phase as an endothermic peak at 145 °C with a weight loss of 7.30% (calculated 7.36%). Weight loss of 26.10% (calculated 26.05%) accompanied by an endothermic peak in a range of 280-295 °C was attributed to the loss of coordinated group 2 (OAc), while the endothermic peak observed at 314 °C is related to the melting point of the complex. The last passage observed as exothermic peaks at 445, 495, 520 and 585 °C with a weight loss of 38.30% (calc. 38.21%), related to the complete decomposition of the exposed complex with formation of CdO. The thermogram of complex (12) showed a six-step decomposition, the first involving the breaking of the H bonds accompanied by an endothermic peak at 49 °C. In the second step, three molecules of hydrated water molecules were lost endothermically, with a peak at 70 °C, accompanied by a weight loss of 11.10% (11.04% calculated). The loss of two coordinated water molecules was recorded in the third step as an endothermic peak at 165 °C with a weight loss of 8.40% (calculated 8.28%). The weight loss of 29.50% (calculated 29.57%) accompanied by an endothermic peak in the range of 270-285 °C was attributed to the loss of coordinated 2(OAc) groups, while the observed endothermic peak at 338 °C indicated the melting point of the complex. The final step, which was observed as exothermic peak at 460, 530, 575 and 615 °C with 26.30% weight loss (Calc 26.33%), referred to a complete decomposition of the complex that was exposed to the formation of NiO. The first step, which was observed in the thermogram of the complex (13), which was accompanied by the endothermic peak at 46 °C. In the second step, three molecules of hydrated water went with a peak at 80 °C Endotherm. Accompanied by % 8.00 (Calc. 8.04 %) weight loss. Weight loss of 18.90% (calculated 18.97%) accompanied by an endothermic peak in a range of 260-280 °C was attributed to the loss of coordinated groups 2 (OAc), while the endothermic peak observed at 340 oC relative was at the point dissolution of the complex. The last passage observed at 445, 490, 540 and 610 °C with a weight loss of 14.60% (calc. 14.68%), relative to the complete oxidative decomposition of the exposed complex with the formation of NiO. The first step observed in the thermogram of complex (15) where the H bonds are broken, accompanied by an endothermic peak at 50 °C. In the second step, three molecules of hydrated water were lost endothermally with a peak at 80 °C accompanied by a weight loss of 8.10% (calculated 8.04%). Weight loss of 19.10% (calculated 19.09%) accompanied by an endothermic peak at 255-275 °C was attributed to the loss of coordinated groups 2 (OAc), while the endothermic peak observed at 330 °C was correlated to the loss of coordinate 2 (OAc) melting point of the complex. The last passage observed at 455, 495, 555 and 620 °C with a weight loss of 14.10% (Calc. 14.20%), refers to the complete oxidative decomposition of the exposed complex with the formation of MnO [54-56].

**Table (6): Thermal analyses for some metal (II) complexes:**

Compound No. Molecular formula	Temp. (°C)	DTA (peak)		TGA (Wt.loss %)		Assignments
		Endo	Exo	Calc	Found	
Complex (2)	46	endo	-	-	-	Broken of H-bondings
	70	endo	-	10.93	10.90	Loss of (3H <sub>2</sub> O) hydrated water molecules
	155	endo	-	8.18	8.10	Loss of (2H <sub>2</sub> O) coordinated water molecule
	270,285	endo	-	29.21	29.25	Loss of coordinated 2(OAc) group
	310	endo	-	-	-	Melting point
	442,495,575,615	-	Exo	27.80	27.70	Decomposition process with the formation of (CuO)
Complex (4)	48	endo	-	-	-	Broken of H-bondings
	75	endo	-	7.35	7.30	Loss of (2H <sub>2</sub> O) hydrated water molecule
	145	endo	-	11.89	12.00	Loss of (3H <sub>2</sub> O) coordinated water molecule
	265	endo	-	24.00	24.10	Loss of coordinated (SO <sub>4</sub> ) group
	315	endo	-	-	-	Melting point
	475,515,590,605	-	Exo	26.15	26.30	Decomposition process with the formation of (CuO)
Complex (5)	50	endo	-	-	-	Broken of H-bondings
	60	endo	-	7.98	7.90	Loss of (3H <sub>2</sub> O) hydrated water molecule
	150	endo	-	2.89	2.80	Loss of (H <sub>2</sub> O) coordinated water molecule
	260,290	endo	-	15.87	15.80	Loss of coordinated SO <sub>4</sub> group
	320	endo	-	-	-	Melting point
	430,465,515,600	-	Exo	15.62	15.60	Decomposition process with the formation of (CuO)
Complex (6)	45	endo	-	-	-	Broken of H-bondings
	80	endo	-	12.08	12.00	Loss of (3H <sub>2</sub> O) hydrated water molecule
	160	endo	-	9.16	9.10	Loss of (H <sub>2</sub> O) coordinated water molecule
	270,285	endo	-	19.89	19.80	Loss of coordinated 2 (Cl) group
	322	endo	-	-	-	Melting point
	435,480,510,595	-	Exo	27.80	27.75	Decomposition process with the formation of (CuO)
Complex (7)	47	endo	-	-	-	Broken of H-bondings
	72	endo	-	8.52	8.60	Loss of (3H <sub>2</sub> O) hydrated water molecule
	273,282	endo	-	12.24	12.20	Loss of coordinated 2 (Cl) group
	325	endo	-	-	-	Melting point
	470,535,600,610	-	Exo	15.62	15.50	Decomposition process with the formation of (CuO)
Complex (8)	46	endo	-	-	-	Broken of H-bondings
	73	endo	-	10.89	10.80	Loss of (3H <sub>2</sub> O) hydrated water molecule
	155	endo	-	8.14	8.10	Loss of (2H <sub>2</sub> O) coordinated water molecule
	260,275	endo	-	29.06	29.10	Loss of coordinated 2(OAc) group
	333	endo	-	-	-	Melting point
	420,480,530,615	-	Exo	28.13	28.20	Decomposition process with the formation of (ZnO)
Complex (9)	49	endo	-	-	-	Broken of H-bondings
	80	endo	-	7.91	7.90	Loss of (3H <sub>2</sub> O) hydrated water molecule
	275,280	endo	-	18.76	18.70	Loss of coordinated 2 (OAc) group
	335	endo	-	-	-	Melting point
	445,490,545,600	-	Exo	15.85	15.80	Decomposition process with the formation of (ZnO)
Complex (10)	45	endo	-	-	-	Broken of H-bondings
	60	endo	-	9.94	9.90	Loss of 3(H <sub>2</sub> O) hydrated water molecules
	145	endo	-	7.36	7.30	Loss of 2(H <sub>2</sub> O) coordinated water molecules
	280,295	endo	-	26.05	26.10	Loss of coordinated 2(OAc) group
	314	endo	-	-	-	Melting point
	445,495,520,585	-	Exo	38.21	38.30	Decomposition process with the formation of (CdO)

### **<sup>1</sup>H-NMR spectra:**

<sup>1</sup>H-NMR spectra of the ligand (**1**) and some of its metal complexes, such as Zn(II) complexes (**8**), (**9**) and Cd(II) complexes (**10**), (**11**). The spectrum of ligand, which showed a peak at 11.220 p.p.m is due to the proton of the aromatic OH group. However, the aromatic ring protons appeared as multiplet peaks in the range 6.902 - 8.057 p.p.m, and another at 9.201 p.p.m corresponds to the proton of the NH<sub>2</sub> group. When deuterated DMSO was used as the solvent, the OH protons disappeared, since D(<sup>2</sup>H) does not appear in the <sup>1</sup>H-NMR spectrum. The protons of the methyl group attached to the carbonyl group appeared at 3.158 p.p.m. The spectrum of the Zn(II) complex (**8**) showed an OH proton at 11.111 p.p.m. The protons of the aromatic rings appeared in the range 6.694 - 8.105 p.p.m and another at 8.991 p.p.m corresponds to proton of the NH<sub>2</sub> group. However, the methyl protons attached to the carbonyl and acetate groups were observed at 3.481 and 1.847 p.p.m respectively. The spectrum of the Zn(II) complex (**9**) showed OH proton at 10.695 p.p.m. The protons of the aromatic rings appeared in the range o 6.799 - 8.103 p.p.m and another at 8.775 p.p.m corresponds to proton of the NH<sub>2</sub> group .However, the methyl protons attached to the carbonyl and acetate groups were observed at 3.155 and 2.501 p.p.m respectively. The spectrum of the Cd(II) complex (**10**) shows OH proton at 10.555 p.p.m. The protons of aromatic rings appeared in the range 6.727 – 7.569 p.p.m and another at 8.565 p.p.m corresponds to proton of the NH<sub>2</sub> group. However the methyl protons attached to the carbonyl and acetate groups were observed at 3.381 and 2.494 p.p.m respectively. The spectrum of the Cd(II) complex (**11**) shows OH proton at 10.765 p.p.m. The protons of the aromatic rings appeared in the range 6.753 – 7.594 p.p.m and another at 8.899 p.p.m corresponds to proton of the NH<sub>2</sub> group. However the methyl protons attached to the carbonyl and acetate groups were observed at 3.391 and 2.499 p.p.m respectively [57].

## Antimicrobial activity:

In vitro biological screening test for ligand (1) and its metal complexes (2), (3), (4), (6), (8), (10), (11), (12) and (14) performed as antibacterial and antifungal activity (Figures 3 and 4). Antibacterial activity was tested against two bacterial strains; Gram-positive *Staphylococcus aureus* as well as Gram-negative strains of *Escherichia coli* [58-60]. The results were compared to the standard drug Ampicillin (Gram positive) and Amphotericin B (Gram negative). The complexes were also shown to have antifungal activity against *Aspergillus flavus* and *Candida albicans* with standard drug. The data indicated that using low concentration against microbes, aspirin and ligand, no effect was observed, however, the complexes show moderate to high effect. The order for Gram positive is Cd(II) complex (10) > Cd(II) complex (11) > ampicillin > Zn(II) complex (8) > Cu(II) complex (4) > Cu(II) complex (6) = Ni(II) complex (12) > Cu(II) complex (2) = Cu(II) complex (3) > ligand(1) > aspirin > Mn(II) complex (14) and for Gram negative is ampicillin > Cd(II) complex (10) > Cd(II) complex (11) > Cu(II) complex (2) > Cu(II) complex (6) > Cu(II) complex (3) > Cu(II) complex (4) > Zn(II) complex (8) > aspirin > Ni(II) complex (12) > ligand (1) > Mn(II) complex (14) and for *Aspergillus flavus* is Cd(II) complex (10) > amphotericin B > Cd(II) complex (11) > ligand (1) = aspirin = Cu(II) complex (2) = Cu(II) complex (3) = Cu(II) complex (4) = Cu(II) complex (6) = Zn(II) complex (8) = Ni(II) complex (12) = Mn(II) complex (14) and for *Candida albicans* is Cd(II) complex (10) > Cd(II) complex (11) > amphotericin B > Ni(II) complex (12) > Cu(II) complex (3) = Cu(II) complex (6) > Cu(II) complex (2) = Cu(II) complex (4) > ligand(1) = aspirin = Zn(II) complex (8) = Mn(II) complex (14). In vivo studies showed no toxicity was observed for all organs tested. "The main groups of antibiotics that are currently in use have three microbial targets: the cell wall synthesis, the translational mechanism and the DNA replication mechanism. Unfortunately, microbial resistance can develop against any of these modes of action. Most of the antibiotic resistance mechanisms are not relevant to nanoparticles (NPs), because the mode of action of NPs is direct contact with the microbial cell wall without the need to penetrate the cell. This raises the hope that NPs are less likely to promote resistance in microbes than antibiotics. Most microbes exist in the form of a biofilm that often contains different species that interact with each other and with their environment. Biofilms are specifically microbial aggregates that rely on a solid surface and extracellular products, such as extracellular polymeric substances (EPSs). Microbes move reversibly on the surface but the expression of EPSs renders the attachment irreversible. Once the microbes have stabilized, the synthesis of the microbial flagellum is inhibited and the microbes multiply rapidly, resulting in the development of a mature biofilm. At this stage, the microbes come together and form a barrier that capable of resisting antibiotics and becoming a source of chronic systemic infections. The biofilm therefore poses a serious threat to health. Nanomaterials are materials that have at least one size (1-100 nm) at the nanoscale. NPs showed broad antimicrobial properties. The antimicrobial mechanism of action of NPs is generally described as following one of three models: oxidative stress induction, metal ion release, or non-oxidative mechanism. These three types of mechanisms can occur simultaneously. Nano Cd(II) complex (10) showed higher activity compared with the standard and other complexes. It may be Cd(II) complex prompt neutralization of the surface electric charge of the microbial membrane and change its penetrability, ultimately leading to microbial death" [61, 62]. The in vitro antibacterial and antifungal activities of the ligand (1), aspirin and some metal complexes are shown in Table (7).

**Table (7): In vitro antibacterial and antifungal activity of ligand (1), aspirin and some metal complexes**

	<i>Escherichia coli</i> (G-)	<i>Staphylococcus aureus</i> (G+)	<i>Aspergillus flavus</i>	<i>Candida</i>
Control: DMSO	0	0	0	0
Ampicillin Antibacterial agent	25	21	0	0
Amphotericin B	0	0	17	21
Aspirin	13	11	0	0
ligand (1)	10	12	0.0	0.0
Cu(II) complex (2)	15	14	0.0	9
Cu (II) complex (3)	14	14	0.0	10
Cu (II) complex (4)	14	16	0.0	9
Cu (II) complex (6)	15	15	0.0	10
Zn (II) complex (8)	14	19	0.0	0.0
Cd (II) complex (10)	24	24	20	26
Cd (II) complex (11)	17	22	17	22
Ni (II) complex (12)	12	15	0.0	17
Mn (II) complex (14)	9	10	0.0	0.0

**Figure (3): In vitro antibacterial and antifungal activity of the ligand (1), aspirin and some metal complexes**



Figure (4): In vitro antibacterial and antifungal diagram of the ligand (1), aspirin and some metal complexes.

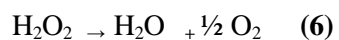
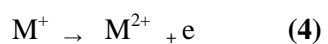
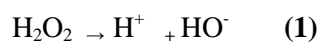
### **In vivo toxicity studies**

The determination of liver functions AST, ALT and albumin in the serum of normal rats did not show significant differences between the treated groups and control groups. Furthermore, there are no any significant differences in renal function or haematological parameters between all groups tested.

### **Catalytic effect:**

The decomposition of  $H_2O_2$  was used as a model for the redox reaction to measure the catalytic effect of the prepared complexes (2), (4), (6), (12) and (14). The decomposition reaction was found to follow a first order reaction kinetics. The decomposition data of  $H_2O_2$  on the tested complexes are shown in Figure (5). The data are plotted as  $\ln a/(a-x)$  versus time, where "a" is the initial concentration of  $H_2O_2$  and "x" is the concentration after time t. the rate constant values for the complexes are 0.014 Cu(II) complex (2), 0.02 Cu(II) complex (6), 0.033 Cu(II) complex (4), .036 Ni(II) complex (12) and 0.043 Mn(II) complex (14) respectively. As shown in Figure (5), although the all complexes are octahedral geometry, the catalytic effect belongs to the nature of the metal ion and anions. Previous studies reported the  $M^{+2}/M^+$  system formed a catalytic active site. The  $M^+$  was identified as the species which controlling the catalytic

activity of the complexes [63]. The order of the catalytic effect is Mn(II) complex (14) > Ni(II) complex (12) > Cu(II) complex (4) > Cu(II) complex (6) > Cu(II) complex (2) respectively. The decomposition of H<sub>2</sub>O<sub>2</sub> in the presence of the complex can be represented as follows:-

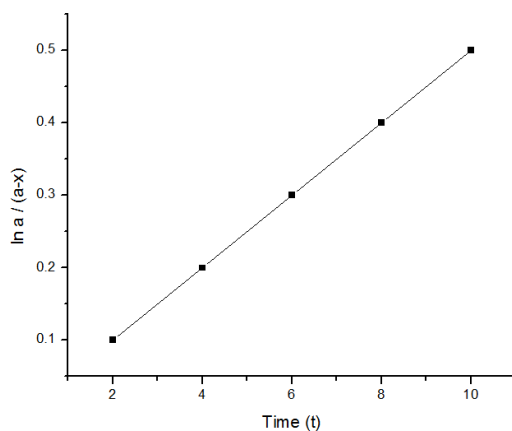


Cu(II) complex (2)

Cu(II) complex (6)

Cu(II) complex (4)

Ni(II) complex (12)



Mn(II) complex (14)

Figure (5):- Decomposition of H<sub>2</sub>O<sub>2</sub> on tested complexes at room temperature.

## **Conclusion**

In this paper, we are trying to focus attention on the synthesis of new compounds. These new compounds have a considerable importance in medicinal chemistry due to their broad spectrum as anti-inflammatory, anti-bacterial and anti-fungal agents. We also give spots on the target compound, complex (10) because of its nano structure which gives it a great possibility to be used as anti-viral drug.

## **Competing interests:**

Authors have declared that no competing interests exist.

## **Funding:**

There is no fund.

## **References:-**

- 1) H. Ilkimen, C. Yenikaya, M. Sart, M. Bulbul, E. Tunca and H. Dal, (2014). Synthesis and characterization of a proton transfer salt between 2,6-pyridinedicarboxylic acid and 2-aminobenzothiazole, and its complexes and their inhibition studies on carbonic anhydrase isoenzymes, *Journal of enzyme inhibition and medicinal chemistry* 29 (3), 353-361.
- 2) M. N. Deodhar, A. C. Dongre and S. D. Kudale, (2012). Analgesic and Antiinflammatory Activity of Derivatives of 2-Aminobenzothiazole *Asian Journal of Chemistry*, 24 (6), 2747- 2752.
- 3) A. Sukul, S. K. Poddar, S. Haque, S. K. Saha, S. C. Das, Z. Al Mahmud and S. M. Adur Rahman, (2017). Synthesis, Characterization and Comparison of Local Analgesic, Anti-Inflammatory, Anti-Ulcerogenic Activity of Copper and Zinc Complexes of Indomethacin. *Anti-inflammatory & Anti-allergy Agents in Medicinal Chemistry*, 15 (3), 221- 233.

- 4) I. Lakovidis, I. Delimaris and S. M. Piperakis, (2011). Copper and Its Complexes in Medicine: A Biochemical Approach, *Molecular Biology International*, vol (2011), 13.
- 5) Thompson, K. H., Orvig, C. (2003). Boon and Bane of Metal Ions in Medicine. *Science*, vol 300 (5621), 936- 939.
- 6) Regiel-Futyra, A., Da browski, J.M., Mazuryk, O., Spiewak, K., Kyzioł, A., Pucelik, B., Brindell, M., Stochel, G. (2017). Bioinorganic antimicrobial strategies in the resistance era, *Coordination Chemistry. Reviews*, 351, 76-117.
- 7) Guerra, W., Silva-Caldeira, P.P., Terenzi, H., Pereira-Maia, E.C. (2016). Impact of metal coordination on the antibiotic and non-antibiotic activities of tetracyclinebased drugs, *Coordination Chemistry. Reviews*, 327-328, 188-199.
- 8) Mohler, J.S., Kolmar, T., Synnatschke, K., Hergert, M., Wilson, L.A., Ramu, S., Elliott, A.G., Blaskovich, M.A.T., Sidjabat, H.E., Paterson, D.L. (2017). Enhancement of antibiotic-activity through complexation with metal ions-combined ITC, NMR, enzymatic and biological studies, *Journal of Inorganic and Biochemistry*, 167, 134-141.
- 9) Yu, M., Nagalingam, G., Ellis, S., Martinez, E., Sintchenko, V., Spain, M., Rutledge, P.J., Todd, M.H., Triccas, J.A. (2016). Nontoxic metal-cyclam complexes, a new class of compounds with potency against drug-resistant *Mycobacterium tuberculosis*, *Journal of Medicinal Chemistry*, (59), (12), 5917-5921.
- 10) Shahabadi, N., Shiri, F., Hadidi, S. (2019). Studies on the interaction of antibiotic drug Rifampin with DNA and influence of bivalent metal ions on binding affinity, *Spectrochim. Acta A Mol. Biomol. Spectrosc*, (219), 195-201.
- 11) Nazir, S., Anwar, J., Munawar, M.A., Qazi, J.I., Best, S.P., Cheah, M. Yaseen, M. (2018). Metal complexation induces antibiotic activity in S-Ethyl-L-Cysteine sulfoxide, *Inorg. Chim. Acta*, (478), 166-175.
- 12) Williamson, K.L., *Macroscale*, M. (1994). *Organic Experiments*, Houghton Mifflin, Boston, Mass, USA, 2nd edition.
- 13) Ngaini, Z., Mohd A.M.A., Hussain, H., Mei, E.S., Tang, D., Kamaluddin, D.H.A. (2012). "Synthesis and antibacterial activity of acetoxybenzoyl thioureas with aryl and amino acid side chains," *Phosphorus, Sulfur and Silicon and the Related Elements*, (187), (1), 1-7.
- 14) Lawal, A., Obaleye, J. A. (2007). "Synthesis, characterization and antibacterial activity of aspirin and paracetamol-metal complexes," *Biokemistri*, (19), (1), 9-15.
- 15) Chavan, A.B., Chitte, P. D., Choudhary, N. P., Albhar, K. G., Hukkeri, V. I. (2012). "Synthesis and biological evaluation of novel benzimidazole derivative with aspirin as potent antimicrobial & antifungal agents," *International Journal of Scientific Research and Reviews*, (1), 22-30.
- 16) Bratasz, K., Selvendiran, T., Wasowicz. (2008). "NCX-4040, a nitric oxide-releasing aspirin, sensitizes drug-resistant human ovarian xenograft tumors to cisplatin by depletion of cellular thiols," *Journal of Translational Medicine*, (6), (9).
- 17) Joseph, S., Nie, T., Huang, L. (2011). "Structure-activity relationship study of novel anticancer aspirin-based compounds," *Molecular Medicine Reports*, (4), (5), 891-899.
- 18) Friedman, A.J., Grote, E.C., Meckfessel, M.H. (2016). Urea: a clinically oriented overview from bench to bedside. *J Drugs Dermatol*, (15), 633-639.
- 19) Voegeli, D. (2012). Urea creams in skin conditions: composition and outcomes. *Dermatol Pract*, (18), 13-15.

- 20) Wohlrab, W. (1984). The influence of urea on the penetration kinetics of topically applied corticosteroids. *Acta Derm Venereol*, (64), 233-238.
- 21) Marion, L.G., Krum, R. (1979). Specialized vehicles to augment percutaneous penetration of topical steroids. *Curr Ther Res*, (25), 56-66.
- 22) Dars, S., Banwell, H.A., Matricciani, L. (2019). The use of urea for the treatment of onychomycosis: a systematic review. *J Foot Ankle Res*, 12-22.
- 23) Vogel, A. (1978). *A Text Book of Quantitative Inorganic Analysis*, London: ELBS.
- 24) Figgis, B., Lewis, J., Wilkins, R. (1960). *Modern Coordination Chemistry*, New York: Interscience.
- 25) Vichai, V., Kirtikara, K. (2006). Sulforhodamine B colorimetric assay for cytotoxicity screening, *Nature Protocols*, 1: 1112-1116.
- 26) Nagesh, G., Mruthyunjayaswamy, B. (2015). Synthesis, characterization and biological relevance of some metal (II) complexes with oxygen, nitrogen and oxygen (ONO) donor Schiff base ligand derived from thiazole and 2-hydroxy- 1-naphthaldehyde, *Journal of Molecular Structure*, 1085: 198-206.
- 27) El-Tabl A. S., Abd-El Wahed M. M., Ahmed, R.A.S., Sarhan, K.S. (2020). Synthesis and structural characterization of new and exciting NP complexes-based paracetamol moiety with antimicrobial activity *Journal of Chemistry and Chemical Sciences*, 10(1), 32-64.
- 28) El-Tabl, A. S., Abd-El Wahed, M.M., Ashour, A.M., Ahmed, R.A.S. (2021). The new acetaminophen drug in the form of nano-organometallic compounds as a bright future for antimicrobial therapy, *Drug designing open access*, 10(2), 174.
- 29) Grün, B., Zeileis, A. (2009). Automatic Generation of Exams in R. *Journal of Statistical Software*, 29(10), 1–14.
- 30) Geary, W. J. (1971). The use of conductivity measurements in organic solvents for the characterisation of coordination compounds, *Coordination Chemistry Reviews*, 7, 81-122.
- 31) Pournalimardan, O., Chamayou, A. C., Janiak, C., Hosseini, M. H. (2007). Hydrazone Schiff-base-manganese(II) complexes: Synthesis, crystal structure and catalytic reactivity, *Inorganica Chimica Acta*, 360, 1599-1608.
- 32) Babu, S. V., Reddy, K. H. (2013). Second derivative spectrophotometric determination of copper (II) using 2-acetylpyridine semicarbazone in biological, leafy vegetable and synthetic alloy samples, *Indian Journal of Advances in Chemical Science*, 1, 105-111.
- 33) Chanu, O. B., Kumar, A., Ahmed, A., Lal, R. (2012). Synthesis and characterisation of heterometallic trinuclear copper(II) and zinc(II) complexes derived from bis (2-hydroxy-1-naphthaldehyde) oxaloyldihydrazone, *Journal of Molecular Structure*, 1007, 257-274.
- 34) Fouda, M. F., Abd-Elzaher, M. M., Shakhofa, M. M., El-Saied, F. A., Ayad, M. I., El Tabl, A. S. (2008). Synthesis and characterization of a hydrazone ligand containing antipyrine and its transition metal complexes, *Journal of Coordination Chemistry*, 61, 1983-1996.
- 35) Gudasi, K.B., Patil, M.S., Vadavi, R.S., Shenoy, R.V., Patil, S.A., Nethaji, M. (2006). X-ray crystal structure of the N-(2-hydroxy- 1-naphthalidene) phenylglycine Schiff base. Synthesis and characterization of its transition metal complexes, *Transition Metal Chemistry*, 31, 580-585.
- 36) Hong, M., Yin, H., Zhang, X., Li, C., Yue, C., Cheng, S. (2013). Di- and tri-organotin (IV) complexes with 2-hydroxy-1-naphthaldehyde 5-chloro-2-hydroxybenzoylhydrazone: Synthesis, characterization and in vitro antitumor activities, *Journal of Organometallic Chemistry*, 724, 23-31.

- 37) El-Wahab, Z.A., Mashaly, M.M., Salman, A., El-Shetary, B., Faheim, A. (2004). Co(II), Ce(III) and UO<sub>2</sub> (VI) bis-salicylatothiosemicarbazide complexes: Binary and ternary complexes, thermal studies and antimicrobial activity, *Spectrochimica Acta Part A: Molecular and Biomolecular Spectroscopy*, 60, 2861-2873.
- 38) El-Tabl, A.S., Shakdofa, M.M. (2013). Metal complexes of N'-(2-hydroxy-5-phenyldiazenyl) benzylideneisonicotinohydrazide: Synthesis, spectroscopic characterization and antimicrobial activity, *Journal of the Serbian Chemical Society*, 78, 39-55.
- 39) Saied, E., Fathy, A., Shakdofa, M.M., El-Tabl, A.S., Abd Elzaher, M.M. (2014). Coordination behaviour of N' 1, N' 4-bis ((1, 5-dimethyl-3-oxo-2-phenyl-2, 3-dihydro-1H-pyrazol-4-yl) methylene) succinohydrazide toward transition metal ions and their antimicrobial activities, *Main Group Chemistry*, 13(2), 87-103.
- 40) El-Tabl, A.S. (2002). Synthesis, characterisation and antimicrobial activity of manganese(II), nickel(II), cobalt(II), copper(II) and zinc(II) complexes of a binucleating tetradentate ligand, *Journal of Chemical Research*, 529-531.
- 41) Xiang, G.Q., Zhang, L.X., Zhang, A.J., Cai, X.Q., Hu, M.L. (2004). 6-(2, 4-Difluorophenyl)-3-(3-methylphenyl)-7H-1, 2, 4-triazolo [3, 4-b][1, 3, 4] thiadiazine, *Acta Crystallographica Section E: Structure Reports Online*, 60, 2249-2251.
- 42) Goel, S., Chandra, S., Dwivedi, S.D. (2013). Synthesis, spectral and biological studies of copper(II) and iron(III) complexes derived from 2-acetyl benzofuran semicarbazone and 2-acetyl benzofuran thiosemicarbazone, *Journal of Saudi Chemical Society*, 1319-6103.
- 43) El-wakiel, N., El-keiy, M., Gaber, M. (2015). Synthesis, spectral, antitumor, antioxidant and antimicrobial studies on Cu(II), Ni(II) and Co (II) complexes of 4-[(1H-Benzoimidazol-2-ylimino)-methyl]-benzene-1, 3-diol, *Spectrochimica Acta Part A: Molecular and Biomolecular Spectroscopy*, 147, 117-123.
- 44) El-Tabl, A.S., El-Enein, S.A. (2007). Reactivity of the new potentially binucleating ligand, 2-(acetichydrazido-N-methylidene- $\alpha$ -naphthol)- benzothiazol, towards manganese(II), nickel(II), cobalt(II), copper(II) and zinc(II) salts, *Journal of Coordination Chemistry*, 57, 281-294.
- 45) El-Tabl, A.S., Shakdofa, M.M.E., Whaba, M.A. (2015). Synthesis, characterization and fungicidal activity of binary and ternary metal(II) complexes derived from 4,4'-((4-nitro-1,2-phenylene) bis(azanylylidene))bis(3-(hydroxyimino)pentan-2-one) *Spectrochimica Acta Part A: Molecular and Biomolecular Spectroscopy*, 136, 1941-1949.
- 46) El-Tabl, A.S., El-Saied, F.A., Ayad, M.I. (2002). Manganese(II), iron(III), cobalt(II), nickel(II), copper(II), zinc(II), and uranyl(VI) complexes of n-(2-furylidene) benzothiazol- 2-ylacetohydrazide, *Synthesis and Reactivity in Inorganic and Metal-Organic Chemistry*, 32, 1189-1203.
- 47) El-Tabl, A.S. (2004). Synthesis and characterization of cobalt(II)/(III), nickel(II) and copper(II) complexes of new 14, 15 and 16-membered macrocyclic ligands, *Bulletin of the Korean Chemical Society*, 25, 1757-1763.
- 48) El-Boraey, H., El-Tabl, A. (2003). Supramolecular copper(II) complexes with tetradentate ketoenamine ligands, *Polish Journal of Chemistry*, 77, 1759-1775.
- 49) Ray, R., Kauffmann, G.B. (1990). An EPR study of copper (II)-substituted biguanide complexes. Part III, *Inorganica Chimica Acta*, 174, 237-244.
- 50) El-Tabl, A.S. (2004). Synthetic and spectroscopic investigations of some transition metal complexes of hydroxy-oxime ligand, *Journal of Chemical Research*, 19-22.

- 51) El-Tabl, A.S. (1997). An esr study of copper(II) complexes of N-hydroxyalkylsalicylideneimines, *Transition Metal Chemistry*, 23, 63-65.
- 52) Al-Hakimi, A.N., Shakdofa, M.M., El-Seidy, A.M., El-Tabl, A.S. (2011). N, N 2-bis (3-((3-hydroxynaphthalen-2-yl) methylene- amino) propyl) phthalamide, *Journal of the Korean Chemical Society*, 55(3), 418-429.
- 53) El-Tabl, A.S. (1997). Synthesis and spectral studies on mononuclear copper (II) complexes of isonitrosoacetylacetone ligand, *Polish Journal of Chemistry*, 71, 1213-1222.
- 54) El-Tabl, A.S., Abou-Sekkina, M. (1999). Preparation and thermophysical properties of new cobalt (II), nickel (II) and copper (II) complexes, *Polish Journal of Chemistry*, 73, 1937-1945.
- 55) El-Tabl, A.S., Abd-El-Wahed, M.M., Refae, R.E.S. (2016). Synthesis, Structural Investigation and Biological Evaluation of New Metal Complexes of 4, 4-((bis (phenylamino) methylene) bis-(azoanylylidene) Bis (hydroxyimino) pentan-2-one Ligand. *Journal of Chemistry and Chemical Sciences*, 6 (2), 109-126.
- 56) EL-Tabl, A.S., Wassel, M.A., and Arafa, M.M. (2017). Preparation and investigation of fulvic acid and its metal derivative complexes with application, *International Journal of Scientific & Engineering Research*, 1663-1679.
- 57) El-Tabl, A.S., Abd-El-Wahed, M.M., El-Saied, S.A.E.R. (2018). Design, Spectroscopic Characterization and Antitumor Action of Synthetic Metal Complexes of Novel BenzohydrazideOxime. *Journal of Chemistry and Chemical Sciences*, 8(8), 1048-1072.
- 58) El-Tabl, A.S., Abd-El-Wahed, M.M., Mosa1, R.M.H. (2019). Novel metal complexes of dehydroacetic acid hydrazone as platforms for hepatocellular carcinoma therapy , *Journal of chemistry and chemical science*, 9(4), 128-152.
- 59) El-Tabl, A.S., Abd-El-Wahed, M.M., El-Henawy, E.M., Abd El-Wahab, O.E., Hashim, S.M.F. (2019).Metal complexes in cancer therapy: Synthesis, spectroscopic characterization and antitumor effect against breast cancer of new dihydroxy phenyl ethylidene amino benzoic acid complexes, *International Journal of Scientific and Engineering Research IJSER*, 10(3),631-645.
- 60) El-Tabl, A.S., Abd-El-Wahed, M.M., Ashour, A.M., Abu setta, M.H.H., Hassanin, O.H., Saad, A.A. (2019). Metallo-organic copper(II) complex in nano size as a new smart therapeutic bomb for hepatocellular carcinoma, *Journal of Chemistry and Chemical Sciences*, 9(1), 33-44.
- 61) El-Tabl, A.S., Shaban, M.T., Abd El-Wahed, N.M. (2019). Novel Metal Complexes as Antimicrobial Agents, Synthesis and Spectroscopic Characterization, *Journal of Chemistry and Chemical Sciences*, 9(3), 74-108.
- 62) El-Tabl, A.S., Abd El-Hamid, I., Abd-El-Wahed, M.M., Ahmed, R.A.S., Ashour, A.M., (2022). Novel nano-metal complexes of modified aspirin as future antimicrobial agents, *International Journal of Pharmaceutical Research*, Vol 14 (1), 85-111.
- 63) EL-Boraey, H and EL-Tabl, A.S, (2003), Supramolecular Copper(II) Complexes with Tetradentate Ketoenamine Ligands, *polish journal of chemistry*, vol 77 (12), 1759-1775.